Comparative Analysis of Deterministic and Random Modulations Based on Mathematical Models of Transmission Errors in Series Communication

Karol Niewiadomski, *Student Member, IEEE*, Robert Smolenski, *Member, IEEE*, Piotr Lezynski, *Senior Member, IEEE*, Jacek Bojarski, David W. P. Thomas, *Senior Member, IEEE*, and Frede Blaabjerg, *Fellow, IEEE*

***Abstract*—In many papers, random modulation of power electronic converters is described as an electromagnetic interference (EMI) mitigation technique, which contributes to the assurance of electromagnetic compatibility (EMC) of systems consisting of power electronic converters and serial transmission-based control and measuring devices. However, experimental results as well as theoretical analyses of physical phenomenon suggest that the EMI reduction is ostensible and results from the measuring procedure adopted in standards. This article presents the first known approach to compare the influence of deterministic and random modulation of transmission errors rate in serial communication systems. The comparison is based on the especially developed mathematical models, which are validated experimentally, using a simple setup with a dc/dc converter injecting a noise into the USB/RS232 converter representing a serial transmission scheme. The comparison reveals that for the studied switching frequency range from 10 kHz to 1 MHz, on average, there is no significant difference between random and deterministic modulations with respect to the probability of error rate in serial communication systems. Thus, in such systems, random modulation should not be considered as a valid EMC-assuring technique.**

***Index Terms*—Bit error rate, computational modeling, deterministic modulation, electromagnetic compatibility (EMC), power electronic converter, random modulation (RanM), statistical analysis, time-domain measurements.**

Manuscript received January 13, 2022; revised March 8, 2022 and April 20, 2022; accepted May 9, 2022. Date of publication May 19, 2022; date of current version June 24, 2022. This work was supported by the European Union's Horizon 2020 Research and Innovation Programme under the Marie Sklodowska-Curie Grant 812391—Smart Cities EMC Network for Training. Recommended for publication by Associate Editor A. Lindemann. *(Corresponding author: Robert Smolenski.)*

Karol Niewiadomski and David W. P. Thomas are with the Department of Electrical Engineering, University of Nottingham, NG7 2RD Nottingham, U.K. (e-mail: karol.niewiadomski@nottingham.ac.uk; dave.thomas@nottingham.ac.uk).

Robert Smolenski and Piotr Lezynski are with the Institute of Automatics, Electronics and Electrical Engineering, University of Zielona Gora, 65-516 Zielona Gora, Poland (e-mail: R.Smolenski@iee.uz.zgora.pl; p.lezynski@iee.uz.zgora.pl).

Jacek Bojarski is with the Division of Mathematical Statistics and Econometrics, University of Zielona Gora, 65-516 Zielona Gora, Poland (e-mail: J.Bojarski@wmie.uz.zgora.pl).

Frede Blaabjerg is with the Department of Energy Technology, Aalborg University, 9220 Aalborg, Denmark (e-mail: fbl@et.aau.dk).

Color versions of one or more figures in this article are available at https://doi.org/10.1109/TPEL.2022.3175737.

Digital Object Identifier 10.1109/TPEL.2022.3175737

I. Introduction

RANDOM modulation (RanM) is often treated as a technique that enables the reduction of electromagnetic interference (EMI) generated by power electronic converters in comparison with deterministic modulation (DetM). Generally, differences between RanM techniques presented in the literature rely on different approaches to spread the interference over a frequency range. Applications to various converter topologies provide different EMI reduction levels. In [1], a buck converter with continuous-time second-order delta–sigma modulation and burst-mode techniques was presented for EMI reduction. Paper [2] presented a review of spread-spectrum-based pulsewidth modulation (PWM) techniques as a cost-effective method to meet EMC standards. In [3], the utilization of a true random number pseudohysteresis controller for RanM has been proposed both to avoid cyberattack on the Internet-of-everything devices and to reduce EMI without degrading converters' performance. The reduction of EMI was validated experimentally on a quasi-Z-source dc–dc converter with four hybrid-GaN high-electron-mobility transistors driven by an FPGA [4]. An enhanced phase-shift algorithm of the frequency modulation was implemented in the parallel–series structure for an *LLC*-resonant converter in [5]. EMI mitigation for the drive system was achieved with uniform distribution pulsewidth modulation strategy, presented in [6].

Many papers concern methods that enable even spreading of the interference over a frequency range. To this end, Dove *et al.* [7] used a method of maximum entropy, Wang *et al.* [8] applied a direct sequence spread spectrum, Li *et al.* [9] used a chaotic sinusoid, Chen *et al.* [10] employed a so-called "uniform distribution" PWM, and Kim *et al.* [11] proposed a spread spectrum technique with random-linear modulation. Previously, in the course of our research, using RanM technique in a standardized arrangement, we have obtained EMI reduction exceeding 20 dB [12].

However, experimental results presented in [13] showed that RanM provides only ostensible reduction of EMI. Indeed, the reduction of EMI measured according to the standards [14] results from the measuring procedure itself and depended on the relationship between converter's switching frequency and the intermediate frequency bandwidth (IF BW) and EMI receiver

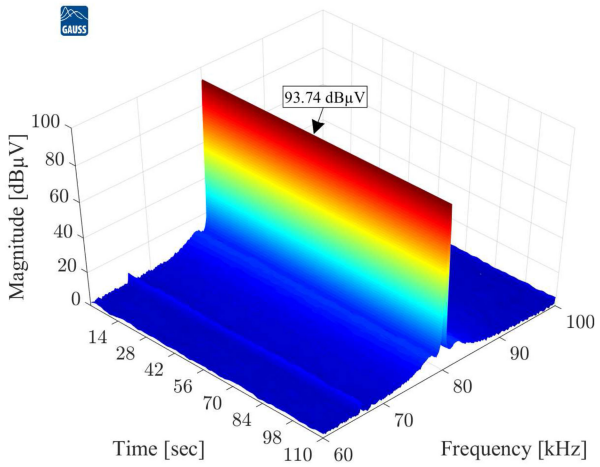

Fig. 1. 3-D spectrogram of EMI measured according to CISPR 11 using the average detector for DetM; switching frequency: 80 kHz.

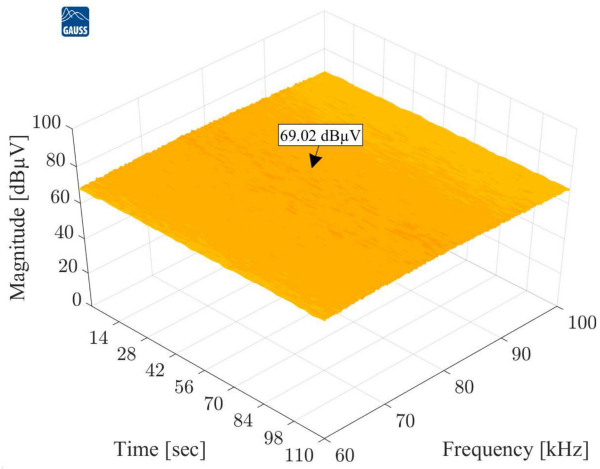

Fig. 2. 3-D spectrogram of EMI measured according to CISPR 11 using the average detector for randomized switching frequency rate of change control algorithm executed with high rate of change; switching frequency randomized symmetrically around 80 kHz.

dwell time. Fig. 1 shows the three-dimensional (3-D) EMI spectrogram measured according to CISPR 11 [14] using a fast digital EMI receiver fully compliant with CISPR 16-1-1 as well as ANSI C63.2 with average detector for DetM with switching frequency equal to 80 kHz. Fig. 2 shows the 3-D EMI for RanM with frequency evenly spread around 80 kHz using an algorithm that controls the rate of change of randomized switching frequency. Fig. 3 shows the same information as presented in Fig. 2 using the same algorithm, but when the rate of change is slower than the dwell time of the digital EMI receiver, it is possible to observe that the reduction of the interference level is ostensible, as it is not connected with random algorithm but depends on the relation between the dwell time of the measuring equipment and the rate of change of the switching frequency. To understand the physical phenomenon underlying such a behavior, a time-domain mathematical model of RanM was developed in [13]. A similar model for a DetM was then developed in [15]. Unfortunately, due to the complexity

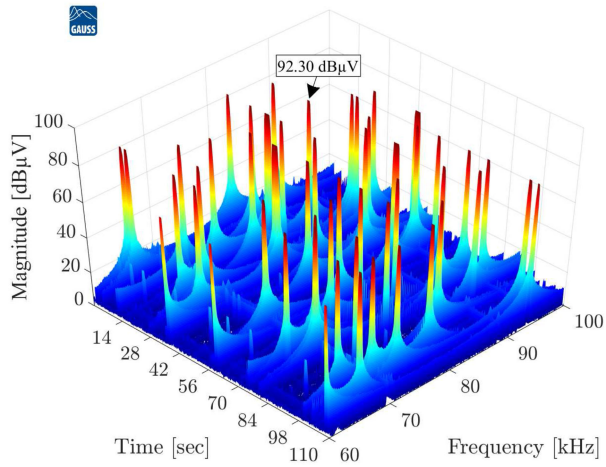

Fig. 3. 3-D spectrogram of EMI measured according to CISPR 11 using the average detector for the same conditions as presented in Fig. 2 for the rate of switching frequency change lower than dwell time of digital EMI receiver; switching frequency randomized symmetrically around 80 kHz.

of the Diophantine equation-based model presented in [15], a direct and unequivocal comparison of DetM and RanM was impossible.

The direct motivation for the concept of these studies was observations from practical *in situ* EMC work. In the system consisting of an ac/dc fast charging station (ChS) and an electric bus, the controller area network (CAN) communication between ChS and the battery management system was disturbed. In this case, the transmission wires of a single-ended unshielded CAN communication were laid along with power wires in the charging cable. Time-domain measurements indicated that a small reduction of interference voltage would assure reliable communication. Based on data provided in the literature, we applied RanM in the ChS converter. Such an approach, according to standardized measurements and literature data, should provide 20 dB (ten times) reduction of EMI. Despite a significantly lower level of interference in the frequency domain, no influence on CAN data transmission errors was observed in the case of RanM. However, a small change of switching frequency in the case of DetM enabled reliable CAN communication. In this article, the explanation of this phenomenon, based on experimental results as well as mathematical models, is presented. Thus, the results provided hereafter are important for both cognitive and practical reasons.

Moreover, in this article, we present the first known attempt to compare the influence of EMI generated by DetM and RanM on serial communication-based devices. Contrary to [16], where authors proposed a hypothesis testing framework that allows to infer the influence of repetitive (thus, only deterministic) electromagnetic disturbances on the series data transmission error, with the usage of Monte Carlo simulation and modified χ^2 test, our comparison is based on two probabilistic mathematical models. The first one, introduced in [13], describes RanM with different parameters, such as bit numbers in transmitted frames, and the second one, based on the Diophantine equation [17], [18], was elaborated for DetM [15]. The second model is enhanced in

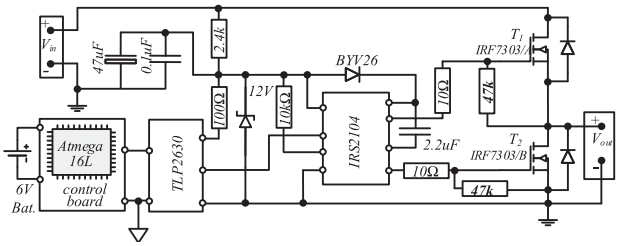

Fig. 4. Schematic of the dc/dc converter used in the measurements.

this article: we provide explicit calculations of the probability of interference for several special cases for DetM, and we show the limitations of the model and the way to overcome those. All of which were not discussed in previous papers. For the comparison between RanM and DetM, we utilize statistical hypothesis testing methods, particularly the proportions test and exact binomial test. Finally, a data averaging procedure is employed, which verifies that there is no significant difference between the probability of interference in systems with either of the two modulation techniques.

II. Standardized Conducted EMI Tests Versus Assessment of EMC of Series Transmission in Presence of EMI

Originally, principles of EMC were focused on the assurance of proper radio-television (RTV) signal reception; hence, the common practice in EMC testing was to evaluate the interference in the frequency domain. In such an approach, for the EMC assessment, it suffices to use a selective superheterodyne receiver, which accurately simulates a typical RTV receiver. Most standards rely on setting limits for particular frequencies. As it has been shown in [19], when measured in the frequency domain, RanM can ostensibly lower the amount of interference by spreading it over the frequency range. Even in recently published papers [20], [21], RanM is perceived as an EMI mitigating technique. However, the experimental results presented in the following show that ordinary standardized EMI measurements are not sufficient, and more in-depth analyzes are required to assure EMC in systems with series communication.

In order to show the influence of the standardized measuring procedure, which utilizes an EMI receiver, an especially developed experiment was conducted using a converter presented in Fig. 4. Measurements have been carried out in a standardized system [14] consisting of a power electronic converter with a switching frequency equal to 6 kHz, in the case of DetM, and evenly dispersed around 6 kHz, in the case of RanM. The 200 final measurements obtained with an average detector with a measuring time equal to 1 s were taken for each investigated case. According to the currently binding standard [14], one final measurement is sufficient for comparison with a limit line for a given frequency. For the measurement, we selected the specific frequency equal to 150 kHz (25th harmonic of the converter's switching frequency), which is a common border frequency for CISPR A (9–150 kHz) and CISPR B (150 kHz–30 MHz) frequency ranges. Both ranges are treated as conducted EMI

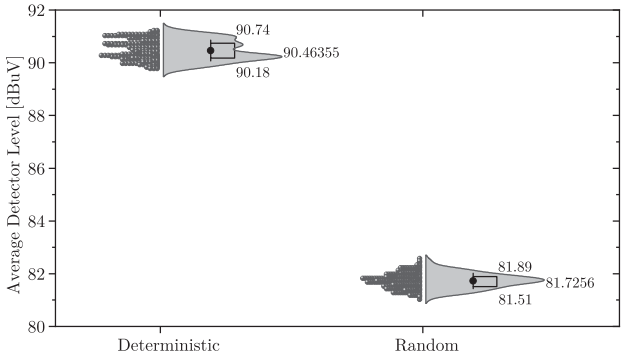

Fig. 5. Half-violin chart of 200 final EMI measurements taken using the average detector for 150 kHz and IF BW = 200 Hz.

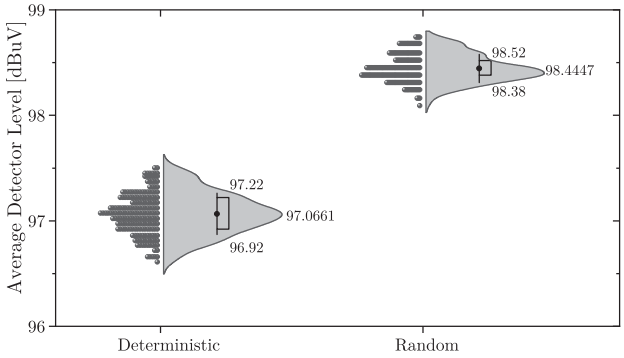

Fig. 6. Half-violin chart of 200 final EMI measurements taken using the average detector for 150 kHz and IF BW = 9 kHz.

ranges; however, different EMI receiver's selectivity settings are demanded. For CISPR A, the IF BW is equal to 200 Hz, while for the CISPR B range, IF BW is equal to 9 kHz. Fig. 5 shows distributions of 200 final measurements for DetM and RanM for 150 kHz, and for IF BW = 200 Hz, while Fig. 6 shows equivalent results for IF BW = 9 kHz. It is easy to observe that in the case of IF BW = 200 Hz, the level of EMI, measured according to the standard, is significantly lower for RanM compared to DetM. In the second case, the measurement indicates that EMI generated by a converter with DetM is slightly lower than that in the case of RanM. This example shows that the interference is influenced by the EMI receiver's selectivity and indicates the necessity of an in-depth analysis of the results. A detailed discussion of this phenomenon has been presented in our earlier paper [19], while a detailed description of the utilized measuring methodology has been provided in [22].

Furthermore, most communication devices or microprocessors used in control and smart metering applications use asymmetric series transmission schemes instead of selective signal receiving. In such a case, a communication signal is established by measuring the voltage to the ground at specific time instants. Therefore, disturbances in such communication systems should be analyzed in the time domain. Disturbances may shift the signal voltage levels causing inaccurate readings and lowering the communication speed. Such a disturbance may occur due to high-frequency EMI currents caused by the pulse mode operation of converters. These currents lead to voltage drops

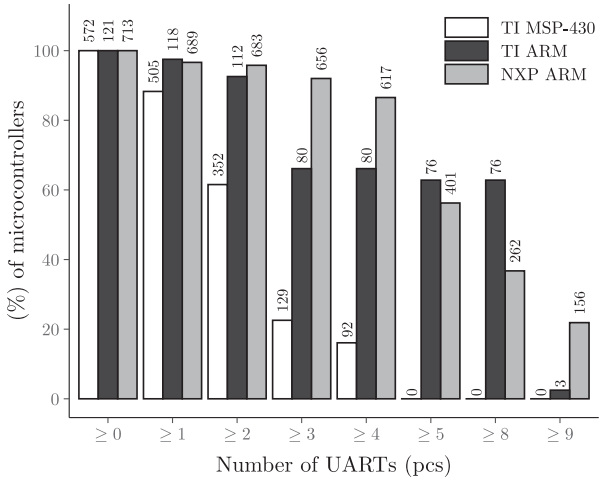

Fig. 7. Percentage of microcontrollers of selected types equipped with UART communication modules, based on: https://www.nxp.com and https://www.ti.com (accessed: January 2022).

on the series circuitry elements, depicted and spread out using common impedance, e.g., PE wires. The most crucial issue to counteract communication interference is to eliminate such electromagnetic coupling, which can be achieved in various ways, for instance, by separating circuits or by applying shields. Electric communication systems can generally be divided into differential signaling circuits (RS-422, RS-485, HDMI, CAN) and single-ended circuits (RS-232, I2C, SPI, UART). Differential signalling uses two complementary signals, which eliminates common impedance coupling and makes communication more resistant to disturbances. Nevertheless, single-ended communication is still commonly used in some parts of the system. An example of single-ended asymmetric communication is the universal asynchronous receiver-transmitter (UART), commonly used in microcontrollers. Fig. 7 shows what percentage of microcontrollers of selected types are equipped with the UART communication module. For example, 118 different ARM microcontrollers manufactured by Texas Instruments are equipped with at least 1 UART module out of all 121 ARM microcontrollers from this manufacturer.

By using additional modules, UART communication may be adjusted to other standards (USB or RS-485). Often, even if we use main transmission links immune to disorders (symmetrical communication, optical fibers, etc.), we still have single-ended parts of the system that might be sensitive to such disorders (short connections, printed boards, signal converters, etc.). Thus, the analyses presented in the article concern a wide range of microprocessor and communication systems.

III. EMC in Series Transmission Systems

In line with the definition of Electromagnetic Compatibility, in the case of serial data transmission, the EMC assessment should focus on assuring a reliable transmission. One possible way of quantifying the transmission reliability is to measure the waiting times for obtaining an error in the reading. To this end, an experiment has been conducted, which employed RanM and

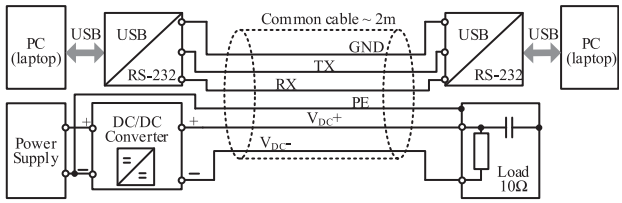

Fig. 8. Schematic of measuring arrangement consisting of the dc/dc converter injecting the noise to the USB/RS-232 converter through common cables.

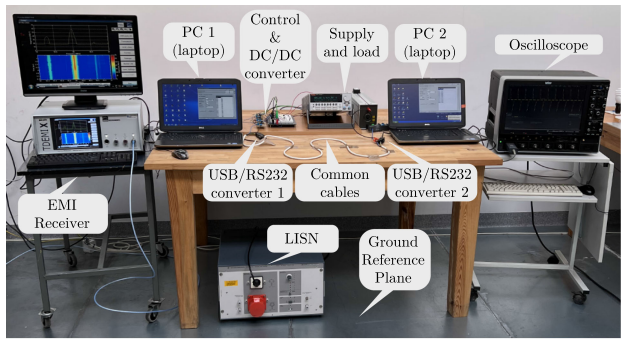

Fig. 9. Laboratory photo of the measuring arrangement from Fig. 8.

TABLE I
Parameters and Results of the Experiment Depicted in Fig. 8 With Transmission Rate 58 409 Hz

f_s (kHz)	Number of sent frames	Number of rejected frames	Probability of error	Mean error awaiting time (s)
Deterministic				
20	1520	330	0.2171	0.5689
21	1515	209	0.1380	0.8993
22	1530	338	0.2209	0.5579
23	1516	420	0.2770	0.4670
24	1511	432	0.2859	0.4367
25	1519	312	0.2054	0.7980
Random				
20	1513	300	0.1983	0.6538
21	1528	327	0.2140	0.5942
22	1515	337	0.2224	0.5814
23	1525	347	0.2275	0.5502
24	1521	378	0.2485	0.5181
25	1517	396	0.2610	0.4684

DetM techniques to drive the DC/DC converter from Fig. 4. The schematic of the test arrangement with interference coupling point has been presented in Fig. 8, while Fig. 9 shows the photo of the laboratory setup with series data transmission system, converter as well as devices for both time (oscilloscope) and frequency (EMI test receiver) domain measurements indicated by appropriate labels. The converter in this arrangement was responsible for providing representative digital signals, e.g., control devices comprising microprocessor-based control. The switching frequency was changed from 20 kHz to 25 kHz with a step of 1 kHz. For RanM, the variance of frequency change was 50%. For each frequency, over 1000 data frames, each consisting of 280 bits, were sent to the RS232/USB converter with a transmission rate equal to ∼58 409 Hz. The exact numbers of the sent data frames are presented in Table I.

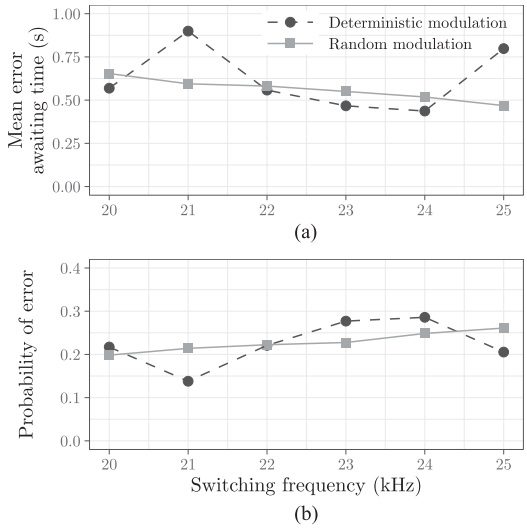

Fig. 10. Results of the experiment from Fig. 8. (a) Mean awaiting times for the transmission error. (b) Probability of the transmission error.

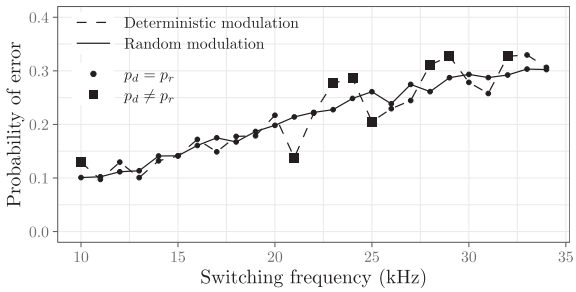

Fig. 11. Probability of errors obtained from the experiment with DetM and RanM.

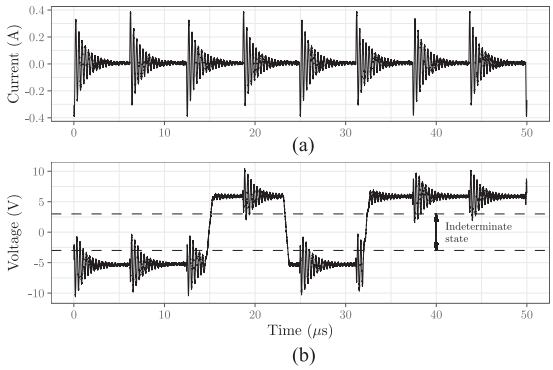

Fig. 12. Waveforms taken in measuring arrangement. (a) EMI current generated by the converter. (b) Serial transmission signal with superimposed interference coupled from the converter.

As a result, many data frames were rejected by the receiving device due to an error in the reading. Table I lists the number of rejected frames as well as the meantime of awaiting for such an error. For a visual comparison, Fig. 10(a) shows the mean error awaiting times as a function of frequency, separately for RanM and DetM. One can observe that there seems to be a decreasing relationship between the mean awaiting time and the switching frequency for RanM. However, no conclusion can be drawn as to the relationship between RanM and DetM. Indeed, by comparing results presented in Table I and Fig. 10(a), one observes that for the switching frequencies of 21 and 25 kHz, the mean awaiting time for an error is larger for DetM than for RanM. For the remaining frequencies, the situation is reversed, that is, the mean awaiting time is higher in RanM case compared to DetM. Since the number of sent frames slightly differs between the cases, in Table I, the frequentist probability of error is introduced as the number of rejected frames over the number of the sent frames. This metric is also depicted in Fig. 10(b). It is easily observed that the probability is directly linked to the mean error awaiting time: the higher the probability, the lower the mean error awaiting time. However, apart from the apparent trend for RanM with respect to the switching frequency, no obvious advantage of using RanM over DetM can be concluded from the collected data. Therefore, to further compare the two modulation techniques, the experiment was repeated to include a wider switching frequency range. Using the same setup and the same data transmission rate, the nominal switching frequency has been changed between 10 and 34 kHz with a step of 1 kHz. As previously, for each frequency, over 1000 data frames, each consisting of 280 bits, were sent to the RS232/USB converter. The discussed experiment can be thought of as a Bernoulli trial, in which the "success" (obtaining the error) is reached with the probability of p, while the "failure" (not obtaining the error) is reached with probability $1 - p$. For a fixed switching frequency, let p_d denote the probability of success in DetM case (thus, $1 - p_d$ being the probability of failure) and p_r denote the probability of success in RanM case (with $1 - p_r$ denoting the probability of failure). The first step of the comparison between the modulation techniques was to verify whether p_d and p_r are significantly different. To this end, the proportions test [23] was employed, and the null hypothesis stated that no significant difference between p_d and p_r can be found. The results of the test are visually presented in Fig. 11. Probabilities p_d and p_r are indicated, respectively, with a dashed and a solid line. Black squares depict the values of p_d for which the null hypothesis was rejected at a significance level $\alpha = 0.05$. Indeed, it is observed that for switching frequencies 10, 21, 23, 24, 25, 28, 29, and 32 kHz, the probabilities of an error differ significantly between the modulation techniques. For the remaining frequencies, no significant difference between RanM and DetM is found.

IV. Statistical Evaluation of Time-Domain Measurements

To understand the differences between the transmission errors in setups using DetM and RanM, one needs to look at the transmitted signals in the time domain. In the applied communication scheme, signals from -3 V down to -5 V correspond to binary "1" and signals from 3 up to 5 V correspond to binary "0." Fig. 12(a) shows the EMI current generated by the switching converter used in the test, measured in PE line in Fig. 8. As it can be seen, a single interference pattern has the shape of a damped oscillation. In our experiment, this shape remained unchanged for both DetM and RanM; only the appearance times

were different. Fig. 12(b) presents the transmission voltage signal with superimposed interference coupled from the converter measured between RX and GND. If the bit checking moment corresponds to the time in which the instantaneous voltage level is located in the indeterminate state zone, depicted in Fig. 12(b), a transmission error occurs and a data frame is rejected. Looking at voltage signals from a time-domain perspective reveals that the only differences between signals present in systems with RanM versus those present in systems with DetM are the time instants at which the interference occurs. Therefore, to accurately compare the two modulation techniques with respect to their capability of assuring the EMC, it is not sufficient to compare the signals in the frequency domain, as in most binding standards, but a time-domain approach is needed alongside. Following these findings, and in order to understand the physical phenomenon underlying such a behavior, two mathematical models for assessing the probability of error were developed in [13] and [15]. The main purpose of the developed models was to obtain an understanding of the considered phenomenon. Furthermore, the models should enable the assessment of data transmission errors based on only a few parameters, namely, the switching frequency, bit checking frequency, and the width of the interference. The first two can be obtained with the knowledge about the system, while the last one is connected with the dominant frequency mode of the interference oscillation and the amplitude of that oscillation and can be derived based on the time-domain measurements. The following sections provide the motivation and a brief overview of the models. It is worth noting that the mathematical models are derived from simplified assumptions, especially since the PWM signal is a square wave with duty cycle equal to 50% or, equivalently, a triangular wave with modulation depth 0.5. It is, therefore, clear that they do not explain all the complex relationships with modulation parameters or electrical parameters of the circuit. However, bearing these limitations in mind, they prove to be useful in the considered context. The extension of these models would greatly complicate the analyses and will be investigated in a frame of future work.

A. Need for a Statistical Approach

As seen in Fig. 12, each switching produces a damped oscillation interference pattern. Therefore, it should be easy to predict the value of this interference at any given point in time. However, this is not the case when the considered system employs the RanM technique. To see why, let us assume for simplicity that in the steady state, the duty cycle $\lambda = 0.5$ is fixed, and let $\Delta S_0 = 1/f_s$ be the nominal switching period. In a deterministic case, roughly after every period $\lambda \Delta S_0$, a new interference pattern should arise. On the contrary, RanM, from a mathematical perspective, can be thought of as a sequence of random variables. Let $\Delta S_1, \ldots, \Delta S_n$ be a sequence of random variables such that ΔS_i follows a uniform distribution $\mathcal{U}((1-\kappa)\Delta S_0, (1+\kappa)\Delta S_0)$ for every $i = 1, \ldots, n$ and $\kappa \in (0, 1)$. A natural question arises: what is the value of the interference after n switching actions? A simple answer is that one cannot directly determine this value. Let us consider the sum $\mathbf{S}_n = \Delta S_1 + \cdots + \Delta S_n$. It easily follows that $\mathbf{S}_n$ is a random variable. Indeed, it can be noticed that $\mathbf{S}_n = (1-\kappa)\Delta S_0 + 2\kappa \Delta S_0 \sum_{i=1}^{n} X_i$, where for each $i = 1, \ldots, n$, random variable X_i follows a standard uniform distribution. The sum $\mathbf{X_n} = \sum_{i=1}^{n} X_i$ is a random variable of Irwin–Hall distribution [24]. From the central limit theorem, it can be concluded that for sufficiently large n (equivalently, sufficiently long time of observation), $\mathbf{X}_n$ approximately follows Normal distribution with mean $n/2$ and variance $n/12$. Thus, random variable $\mathbf{S}_n$ follows approximately Normal distribution with mean $\Delta S_0 - (1-n)\kappa \Delta S_0$ and variance $n\Delta S_0 \kappa/6$. This shows that in RanM, given the nominal switching frequency and a starting point, one cannot directly predict a value of the interference at a particular moment in the future. The above reasoning highlights the need for a statistical approach of predicting the probability of errors. Such an approach has been taken in [13], where a model for predicting the probability of errors has been developed for the RanM scheme. This model will now be briefly recalled.

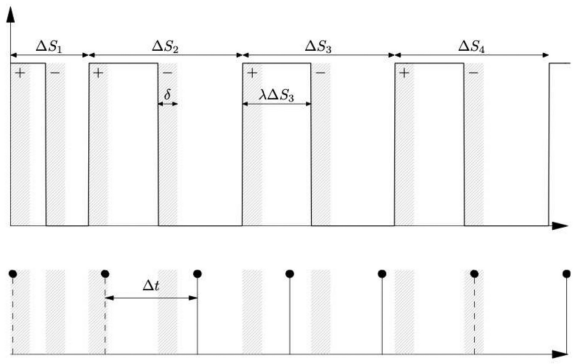

Fig. 13. Visual interpretation of the RanM scheme used in developing the RanM mathematical model.

B. Probability of Error in Systems With RanM

1) Let ΔS_0 be the reciprocal of the nominal switching frequency, i.e., the nominal switching period.
2) Let ΔS_i for $i = 1, 2, \ldots$ be a sequence of random variables following the uniform distribution $\mathcal{U}((1-\kappa)\Delta S_0, (1+\kappa)\Delta S_0)$, where $\kappa \in (0, 1)$.
3) Let Δt be the difference between bit checking moments.
4) Let λ be the duty cycle of the carrier wave.
5) Let δ be the width of the interference, i.e., the period for which the interference signal exceeds a certain predefined threshold.

Fig. 13 visually presents the above parameters. Additionally, the gray stripe, representing the width δ of the interference signal, is classified into two classes, indicated by "+" and "−" signs. The part indicated by "+" represents the signal being above the 2 V threshold. It is understood that in such a case an error in the reading may occur if the value of the bit is 1. Similarly, only if a bit with value 0 overlaps with the "−" interference, the bit value will be corrupted. Let the probability of the occurrence of interference signal "+" be denoted by p and the probability of appearance of bit 1 be denoted by q. Since the event of the occurrence of either "+" or "−" interference

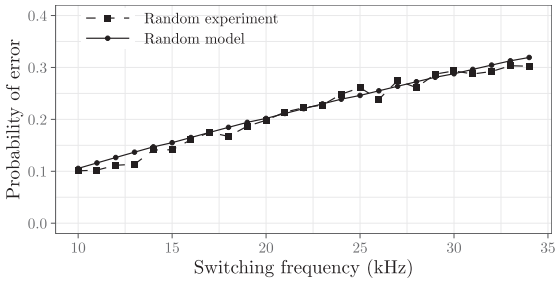

Fig. 14. Predictions of RanM mathematical model versus the experimental results in the RanM case.

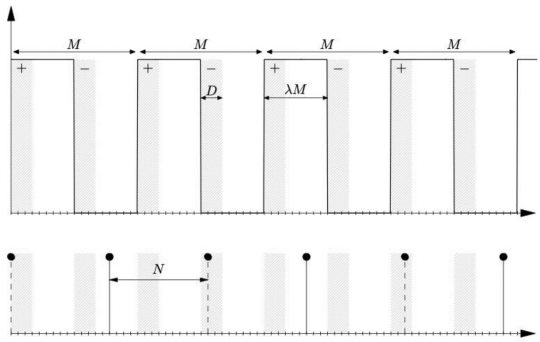

Fig. 15. Visual interpretation of the DetM scheme used in developing the DetM mathematical model.

and the event of occurrence of 1 or 0 value are independent, the probability of the bit corruption p_c is their join probability and can be calculated as $p_c = q + p - 2pq$. A natural assumption is that bits 0 and 1 occur with the same probability, i.e., $q = 1/2$. In such a case, the probability of a single bit corruption p_c is equal to $1/2$, which will be the value used throughout the remainder of this article.

In the experimental case, the error was due to rejection of the whole data frame, which, in the simplest arrangement, may occur even if only one bit in the frame is corrupted. Therefore, the interest is in the prediction of rejection of the whole frame consisting of n bits. Let X be the random variable indicating the number of bits appearing in any of the distorted zones of length δ. The probability of frame rejection is, thus

$$P_{\text{error}} = \sum_{i=1}^{n} \left(1 - (1 - p_c)^i\right) P(X = i) \tag{1}$$

where $P(X = i)$ represents the probability that i bits in the n-bit frame will appear in the distorted signal zone, while the term $1 - (1 - p_c)^i$ represents the total probability with which at least one bit out of i will be corrupted. Let $p_0 = 2\delta/\Delta t$ and $n_0 = \lfloor n\Delta t/\Delta S_0 \rfloor$. It has been shown that for sufficiently large n and $\kappa > 0.25$, the probability of the appearance of the ith bit in the distorted signal zone may be approximated by

$$P(X = i) = \begin{cases} \binom{n_0}{i} p_0^i (1 - p_0)^{n_0 - i} & \text{for } i = 1, \ldots, n_0 \\ 0 & \text{for } i > n_0 \end{cases}. \tag{2}$$

Combining (1) and (2) with the previously made assumptions and after simplification, the final formula of the probability of the frame rejection can be written as

$$P_{\text{error}} \approx 1 - \left(1 - \frac{\delta}{\Delta t}\right)^{\left\lfloor n \frac{\Delta t}{\Delta S_0} \right\rfloor}. \tag{3}$$

Fig. 14 presents the application of the developed model to the data obtained from the experiment. It is easily observed that the model fits the data with satisfying accuracy. Slight deviations are the results of too few repetitions of the experiment.

C. Probability of Error in Systems With DetM

An interesting observation, indicated in Fig. 11, is that in the case of DetM, the behavior is highly complex. That is, the trend resembles that of RanM, but for several switching frequencies, the probability of frame rejection drastically drops. Intuition is that such a behavior is strongly connected with the relationship between the switching frequency and bit checking frequency. One could use number theory in order to obtain a better understanding of the underlying phenomenon. This section gives a brief overview of the deterministic model developed in [15].

Needless to say, every digital device used for measuring signals in the time domain has its own granularity, that is a time step with which the data are collected. Suppose that this time step is fixed and denoted by τ. Any point in time t can then be represented as

$$t = T\tau, \text{ for } T = 0, 1, \ldots. \tag{4}$$

With such an assumption, instead of thinking of the relationship between the switching frequency and bit checking frequency in terms of real-valued functions, one can switch to the field of number theory and think of that in terms of the relationship between integers. Indeed, let $M, N, D \in \mathbf{Z}$ be such that:

1) $\Delta S_0 = M\tau$ is the switching period of the converter with DetM;
2) $\Delta t = N\tau$ is the time between successive bit checking moments;
3) $\delta = D\tau$ is the width of the interference.

Further, let $i = 0, 1, \ldots$ be such that Mi is the time moment of the ith switching-ON of the converter, and let $j = 0, \ldots, n-1$ be such that Nj is the appearance of the jth bit. Moreover, let us denote by $t = 1 - M, 2 - M, \ldots, 0$ the start of the converter switching and let $d = 0, \ldots, D - 1$ be the dth time instant of the interference within the distorted signal zone D. Finally, let λ be the duty cycle of the carrier wave such that $\lambda M \in \mathbf{Z}$. The above assumptions are depicted in Fig. 15. The first question is how to predict the moments at which the interference signal meets the bit value. It has been shown in [15] that in order for such a meeting to occur, the following Diophantine equation need be satisfied:

$$Nj - M\left(\lambda(i \bmod 2) + \lfloor i/2 \rfloor\right) - t - d = 0 \tag{5}$$

for $j = 0, 1, \ldots, n-1$, $d = 0, 1, \ldots, D-1$, and $t = 1 - M, 2 - M, \ldots, 0$. Let $L(t_0)$ denote the number of quadruples (i, j, d, t) satisfying (5) with $t = t_0$. For several specific cases, $L(t_0)$ can be derived analytically; however, in general, there is no formula and computing $L(t_0)$ requires numerical simulations. Under the assumption that bit values 0 or 1 appear with the same probability $1/2$ and from the theorem of total probability,

the probability of frame rejection in the deterministic case can be estimated from the following equation:

$$P_{\text{error}} = 1 - \frac{1}{M} \sum_{t_0=1-M}^{0} \left(\frac{1}{2}\right)^{L(t_0)}. \tag{6}$$

Since, for the specific cases, the value of $L(t_0)$ can be derived, so can be the probability. Those cases will be provided next.

1) N is a Multiplication of M: Let us assume that for some $m \in \mathbf{Z}$, we have $N = mM$. In such case for $t_0 = 1 - M + d$ and $t_0 = 1 - (1 - \lambda)M + d$, where $d = 0, 1 \ldots, D - 1$, all the n bits will be present in the interference zone. Thus, one has

$$\begin{aligned} P_{\text{error}} &= 1 - \frac{1}{M}\left(2D\left(\frac{1}{2}\right)^{n} + (M - 2D)\right) \\ &= \frac{D}{M}\left(2 - \frac{1}{2^{n-1}}\right). \end{aligned} \tag{7}$$

Note that for a fixed frame length n and interference width δ, the above-mentioned case provides a model linearly dependent on the switching frequency.

2) M is a Multiplication of N: Similarly, let $M = mN$ for some even $m \in \mathbf{Z}$. For the value t_0 for which the first bit meets the interference zone, one finds that the successive $2n/m$ bits are also present in the interference zone. Such a situation happens for mD different positions of t_0. For the remaining $M - mD$ positions, $L(t_0) = 0$. Thus, one has

$$\begin{aligned} P_{\text{error}} &= 1 - \frac{1}{M}\left(mD\left(\frac{1}{2}\right)^{2n/m} + (M - mD)\right) \\ &= \frac{D}{N}\left(1 - \frac{1}{4^{n/m}}\right). \end{aligned} \tag{8}$$

An immediate comment is that in this case the dependence is no longer linear because $m = M/N$.

3) N and M are Coprime: Two numbers N and M are coprime if their greatest common divisor is 1. In such a case, their lowest common multiple is simply the product NM. Thus, assuming that first bit and first switching instant occur at the same time, the $(M + 1)$th bit and the Nth switching instant will also occur at the same time. Between these two instants, D bits will be present in the interference zone, thus $L(t_0) = D$. With an additional assumption that the number of bits in the frame n is a multiple of M, i.e.,$n = kM$ for some $k \in \mathbf{Z}$, the probability of frame rejection can be expressed as

$$\begin{aligned} P_{\text{error}} &= 1 - \frac{1}{M} \sum_{t_0=1-M}^{0} \left(\frac{1}{2}\right)^{\frac{D}{M}n} \\ &= 1 - \left(\frac{1}{2}\right)^{\frac{D}{M}n}. \end{aligned} \tag{9}$$

Fig. 16 shows the predictions of the deterministic model overlaid with the experimental probabilities. It can be observed that the trend is preserved, and that for certain switching frequencies, predictions of the model are significantly lower than the trend. However, it can also be seen that unlike in the RanM case, the deterministic model does not align as well with the experimental data. This issue will be tackled in Section V.

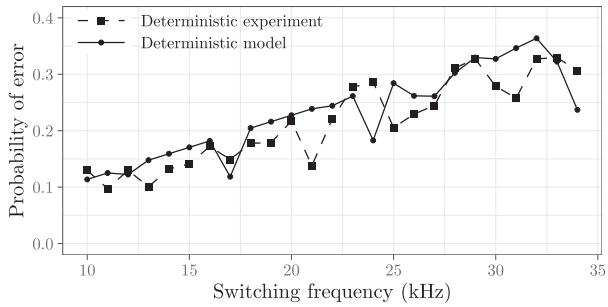

Fig. 16. Predictions of the DetM mathematical model versus results of the experimental investigation for DetM case.

TABLE II
RESULTS OF EXACT BINOMIAL TEST FOR THE FREQUENCIES FOR WHICH $p_d \neq p_r$

f_s (kHz)	Experiment	Prediction	95% CI	p-value
Deterministic				
10	0.1295	0.1120	(0.116, 0.145)	0.0339
21	0.1380	0.2352	(0.124, 0.153)	$< 10^{-6}$
23	0.2770	0.2576	(0.258, 0.297)	0.0885
24	0.2859	0.2228	(0.267, 0.306)	$< 10^{-6}$
25	0.2054	0.1950	(0.188, 0.223)	0.3154
28	0.3112	0.3136	(0.292, 0.331)	0.8683
29	0.3272	0.3248	(0.307, 0.348)	0.8482
32	0.3272	0.3584	(0.307, 0.348)	0.0111
Random				
10	0.1009	0.1056	(0.088, 0.114)	0.5870
21	0.2140	0.2113	(0.197, 0.232)	0.8021
23	0.2275	0.2298	(0.21, 0.246)	0.8551
24	0.2485	0.2389	(0.23, 0.267)	0.3832
25	0.2610	0.2461	(0.243, 0.28)	0.1798
28	0.2612	0.2725	(0.243, 0.28)	0.3412
29	0.2872	0.2810	(0.268, 0.307)	0.5885
32	0.2922	0.3046	(0.273, 0.312)	0.3020

V. COMPARISON OF RANM AND DETM

Comparison of the modulation techniques will be carried out on the basis of the developed models. In the investigated case, we will start by looking at the switching frequencies 10, 21, 23, 24, 25, 28, 29, and 32 kHz for which the errors obtained in the experiment were found to be significantly different, as discussed in Section IV. The conclusion for the rest of the investigated switching frequencies is that there is no direct advantage of using RanM over DetM. First, in order to verify whether the developed models provide a good technique for modeling the rejection probability, an exact binomial test was conducted. The null hypothesis was that the probability predicted by the model is equal to the one obtained from experiments versus the alternative that the two are different. The test for each frequency was conducted at the significance level $\alpha = 0.05$. Table II collects the results of the test for the investigated frequencies. As it is seen, in the case of the random model, p-value indicates that in all cases the null hypothesis is accepted (p-value > 0.05). However, in the deterministic model, the null hypothesis should be rejected for the following switching frequencies: 10, 21, 24, and 32 kHz. The computed p-values indicate that the deterministic model predictions are particularly poor for frequencies 21 and 24 kHz (p-value $< 10^{-6}$).

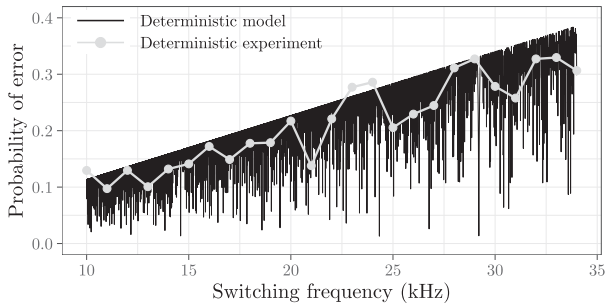

Fig. 17. Predictions of the deterministic model simulated with a small frequency step.

TABLE III
EXACT BINOMIAL TEST FOR FREQUENCIES HIGHER AND LOWER THAN 21 AND 24 KHZ FOR WHICH p-VALUE $< 10^{-6}$ IN THE DETERMINISTIC CASE

f_s (Hz)	Experiment	Prediction	95% CI	p-value
Deterministic				
21000	0.1380	0.2352	(0.121, 0.156)	$< 10^{-6}$
20913		0.1297		0.3390
21014		0.1456		0.4229
24000	0.2859	0.2228	(0.263, 0.309)	$< 10^{-6}$
23993		0.2687		0.1314
24003		0.2688		0.1389
Random				
21000	0.2140	0.2113	(0.194, 0.235)	0.8021
20913		0.2113		0.8021
21014		0.2113		0.8021
24000	0.2485	0.2389	(0.227, 0.271)	0.3832
23993		0.2389		0.3832
24003		0.2389		0.3832

The analysis of the deterministic model allows to understand that it is dependent on the granularity, which affects the relationship between M, N, and D. A small change in one of the parameters results in different predictions. This is shown in Fig. 17, where the deterministic model was simulated for small changes in the switching frequency. As it can be seen, a small change in the switching frequency may lead to a significantly different probability prediction. This leads to the hypothesis that in the cases where p-value was below the significance level α, the actual switching frequency was different from the assumed one. Table III presents the results of a simple brute-force analysis around the frequencies 21 and 24 kHz, for which the p-value obtained in the exact binomial test was the smallest. The analysis consisted of the following steps.

1) For a chosen τ and switching frequency f_s, calculate the integer M.
2) For the specific M, compute the error probability using (2).
3) Apply the exact binomial test for the newly predicted probability and experimental probability.
4) If the computed p-value is less than a significance level α, go to the last step.
5) Increase (decrease) M and repeat previous steps.
6) Calculate new switching frequency f_s from M and compute the prediction of the RanM model for that switching frequency.

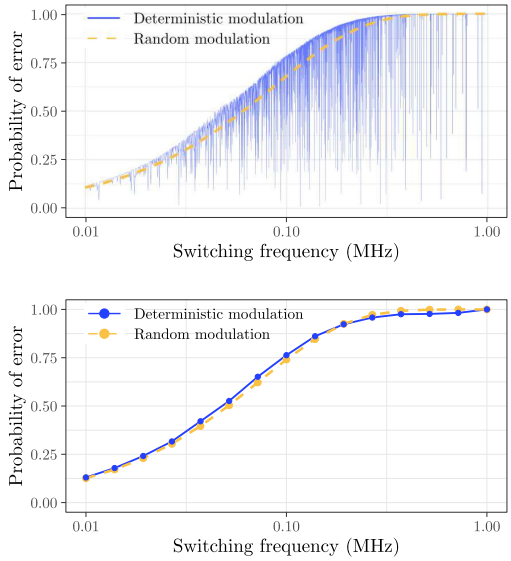

Fig. 18. Average trend of the error probability predictions of the RanM and DetM mathematical models.

The analysis indicates that it is possible to find frequencies both below and above the stated switching frequency for which predictions of the model are close to the experimental probabilities. One may conclude that the actual switching frequency was different from the stated one, either due to imprecise measurement, human error or simply due to switching tolerances inherently associated with the transistors. It is important to point out that the differences in frequencies seen in Table III do not exceed 100 Hz. Thus, instead of 21 kHz, the switching frequency might have been 20 913 or 21 014 Hz, and instead of 24 kHz, the actual switching frequency might have been 23 993 or 24 003 Hz. It is also observed that the predictions of the random model do not differ up to four digits from the ones obtained with stated switching frequencies 21 and 24 kHz, which confirms the choice of the "new" switching frequencies. Accordingly, knowing that the deterministic model is very sensitive to small changes, its application should embrace providing uncertainty bounds, within which the nominal switching frequency may change.

Furthermore, it is evident that a comparison between modulation techniques cannot be carried out by comparing the values at specific frequencies. Fig. 18(a) presents a visual comparison between the models for a wider frequency range 10 kHz–1 MHz with fixed parameters $\Delta t \approx 17.12\,\mu$s, $\delta \approx 40.6$ ns, and $\tau = 1$ ns, corresponding to the ones obtained in the experiment. As already discussed, the complexity of the deterministic model does not allow for an unequivocal comparison. In particular, one may be misled to think that the DetM offers a higher probability of error, judging from the apparent "worst-case" trend in Fig. 18(a). Therefore, an averaging scheme should be used for the models. Fig. 18(b) presents the comparison between the two modulation schemes, with dots connected by a dashed line indicating RanM and dots connected with a solid line representing DetM. The data have been averaged using a simple arithmetic mean with logarithmic differences between the frequencies. As expected,

the results indicate that, on average, there is no significant difference between RanM and DetM in the investigated switching frequency range in the context of the influence of generated EMI on the reliability of serial transmission.

VI. Conclusion

In this article, the first known approach to compare the influence of EMI generated by deterministic and random modulated converters on the probability of error appearance in single-ended serial transmission has been presented. The experimental results of transmission error rates for different converter switching frequencies have not provided unequivocal evidence about the advantage of RanM in the context of serial transmission reliability assurance.

The revealed complexity of the DetM model resulting from number theory indicated strong interdependence between converter switching frequency and the probability of error appearance, confirming that the direct comparison of experimentally obtained results is not possible. The presented models for assessing the probability of errors in systems using random and DetM were derived for simplified assumptions. Even though they provided a good insight into the considered phenomenon and were successfully employed for the prediction of the probability of errors, further work may be needed to account for more complex assumptions, such as different modulation depths. The analysis presented in Table III used a time-consuming brute-force algorithm, which could be optimized in order to be used in real-time systems. Moreover, a direct link could be provided between the *RLC* characteristics of a given device and the width of the interference, for instance, by deriving surrogate circuit models, with the help of stochastic techniques, such as polynomial chaos or support vector machine [25].

The averaging method proposed in this article enabled direct comparison between the modulation techniques on the basis of the simulation results obtained from the mathematical models. Based on the approach proposed in this article, it has been confirmed that in spite of the lower levels of disturbance measured according to the standards, RanM has (on average) no advantage over DetM in the context of EMI influence on serial transmission reliability. Even though similar results have been intuitively understood by other researchers, this article provides the first known mathematical confirmation of it, which is one of the practical aspects of this research and should be taken into account by the EMC/PE engineers or system integrators who are willing to incorporate RanM into their designs. Additionally, the developed model (based on the analysis of the phenomenon) explains why in the case of DetM, a slight change in the switching frequency may contribute to a significant decrease in the transmission error rate and, in some cases, can be used for reliable transmission assurance. This observation has been confirmed in many practical cases.

References

[1] J.-J. Chen, Y.-S. Hwang, C.-S. Jheng, Y.-T. Ku, and C.-C. Yu, "A low-electromagnetic-interference buck converter with continuous-time delta-sigma-modulation and burst-mode techniques," *IEEE Trans. Ind. Electron.*, vol. 65, no. 9, pp. 6860–6869, Sep. 2018.

[2] R. Gamoudi, D. Elhak Chariag, and L. Sbita, "A review of spread-spectrum-based PWM techniques—A novel fast digital implementation," *IEEE Trans. Power Electron.*, vol. 33, no. 12, pp. 10292–10307, Dec. 2018.

[3] W.-H. Yang *et al.*, "A true-random-number-based pseudohysteresis controller for buck DC–DC converter in high-security Internet-of-everything devices," *IEEE Trans. Power Electron.*, vol. 35, no. 3, pp. 2969–2978, Mar. 2020.

[4] S. U. Hasan and G. E. Town, "An aperiodic modulation method to mitigate electromagnetic interference in impedance source DC–DC converters," *IEEE Trans. Power Electron.*, vol. 33, no. 9, pp. 7601–7608, Sep. 2018.

[5] H.-P. Park, M. Kim, and J.-H. Jung, "Spread spectrum technique to reduce EMI emission for an LLC resonant converter using a hybrid modulation method," *IEEE Trans. Power Electron.*, vol. 33, no. 5, pp. 3717–3721, May 2018.

[6] Z. Wang, Y. Xu, P. Liu, Y. Zhang, and J. He, "Zero-voltage-Switching current source inverter fed PMSM drives with reduced EMI," *IEEE Trans. Power Electron.*, vol. 36, no. 1, pp. 761–771, Jan. 2021.

[7] A. Dove, J. Naudé, and I. Hofsajer, "An argument for the relationship between spectral spreading and probability spreading for EMI-reduction in DC–DC converter," *IEEE Trans. Power Electron.*, vol. 35, no. 2, pp. 1459–1472, Feb. 2020.

[8] R. Wang, Z. Lin, J. Du, J. Wu, and X. He, "Direct sequence spread spectrum-based PWM strategy for harmonic reduction and communication," *IEEE Trans. Power Electron.*, vol. 32, no. 6, pp. 4455–4465, Jun. 2017.

[9] H. Li, Z. Yang, B. Wang, V. G. Agelidis, and B. Zhang, "On thermal impact of chaotic frequency modulation SPWM techniques," *IEEE Trans. Ind. Electron.*, vol. 64, no. 3, pp. 2032–2043, Mar. 2017.

[10] J. Chen, D. Jiang, Z. Shen, W. Sun, and Z. Fang, "Uniform distribution pulsewidth modulation strategy for three-phase converters to reduce conducted EMI and switching loss," *IEEE Trans. Ind. Electron.*, vol. 67, no. 8, pp. 6215–6226, Aug. 2020.

[11] M. Kim, H.-P. Park, and J.-H. Jung, "Spread spectrum technique with random-linear modulation for EMI mitigation and audible noise elimination in IH appliances," *IEEE Trans. Ind. Electron.*, vol. 69, no. 8, pp. 8589–8593, Aug. 2022.

[12] H. Loschi, P. Lezynski, R. Smolenski, D. Nascimento, and W. Sleszynski, "FPGA-based system for electromagnetic interference evaluation in random modulated DC/DC converters," *Energies*, vol. 13, no. 9, May 2020, Art. no. 2389.

[13] R. Smolenski, J. Bojarski, A. Kempski, and P. Lezynski, "Time-domain-based assessment of data transmission error probability in smart grids with electromagnetic interference," *IEEE Trans. Ind. Electron.*, vol. 61, no. 4, pp. 1882–1890, May 2014.

[14] CENELEC, "Industrial, scientific and medical equipment—radio-frequency disturbance characteristics—limits and methods of measurement," EN 55011:2016, 2016.

[15] R. Smolenski, J. Bojarski, P. Lezynski, and Z. Sadowski, "Diophantine equation based model of data transmission errors caused by interference generated by DC-DC converters with deterministic modulation," *Bull. Polish Acad. Sci., Tech. Sci.*, vol. 64, no. 3, pp. 575–580, Sep. 2016.

[16] K.-J. Li, Y.-Z. Xie, F. Zhang, and Y.-H. Chen, "Statistical inference of serial communication errors caused by repetitive electromagnetic disturbances," *IEEE Trans. Electromagn. Compat.*, vol. 62, no. 4, pp. 1160–1168, Aug. 2020.

[17] M. R. Nasiri, S. Farhangi, and J. Rodríguez, "Model predictive control of a multilevel CHB STATCOM in wind farm application using diophantine equations," *IEEE Trans. Ind. Electron.*, vol. 66, no. 2, pp. 1213–1223, Feb. 2019.

[18] X. Liu *et al.*, "A fast finite-level-state model predictive control strategy for sensorless modular multilevel converter," *IEEE Trans. Emerg. Sel. Topics Power Electron.*, vol. 9, no. 3, pp. 3570–3581, Jun. 2021.

[19] P. Lezynski, R. Smolenski, H. Loschi, D. Thomas, and N. Moonen, "A novel method for EMI evaluation in random modulated power electronic converters," *Measurement*, vol. 151, Feb. 2020, Art. no. 107098.

[20] C.-H. Moon, C.-J. Chen, and S.-W. Lee, "A random modulation spread-spectrum digital PWM for a low system clock digital buck converter," *IEEE Access*, vol. 9, pp. 156663–156671, 2021.

[21] M. Kim, H.-P. Park, and J.-H. Jung, "Spread spectrum technique with random-linear modulation for EMI mitigation and audible noise elimination in IH appliances," *IEEE Trans. Ind. Electron.*, vol. 69, no. 8, pp. 8589–8593, Aug. 2022.

[22] R. Smolenski, *Conducted Electromagnetic Interference (EMI) in Smart Grids* (Ser. Power Systems). London, U.K.: Springer-Verlag, 2012.

[23] R. G. Newcombe, "Interval estimation for the difference between independent proportions: Comparison of eleven methods," *Statist. Med.*, vol. 17, no. 8, pp. 873–890, Apr. 1998.
[24] P. Hall, "The distribution of means for samples of size N drawn from a population in which the variate takes values between 0 and 1, all such values being equally probable," *Biometrika*, vol. 19, no. 3/4, pp. 240–244, Dec. 1927.
[25] K. Niewiadomski, S. Sumsurooah, and D. W. P. Thomas, "Comparison of selected support vector machine approaches for stochastic power electronic circuit simulation with parasitics," in *Proc. IEEE Int. Joint EMC/SI/PI EMC Europe Symp.*, 2021, pp. 591–596.

Karol Niewiadomski (Student Member, IEEE) was born in 1995 in Zielona Gora, Poland. He received the Engineering degree in 2018 and the M.Sc. degree in 2019 in data engineering from the University of Zielona Gora, Zielona Gora, Poland. He is currently working toward a joint Ph.D. degree in electrical engineering with the George Green Institute for Electromagnetic Research, University of Nottingham, Nottingham, U.K.

His research interests include uncertainty analysis, machine learning, statistical analysis, and their application to electrical engineering.

Robert Smolenski (Member, IEEE) was born in 1973 in Krosno Odrzanskie, Poland. He received the M.Sc., Ph.D., and Postdoctoral degrees in electrical engineering from the University of Zielona Gora, Zielona Gora, Poland.

He is currently an Associate Professor and the Head of the Institute of Automatics, Electronics and Electrical Engineering, University of Zielona Gora, and the Deputy Chair of the Joint IEEE IES/PELS Poland Chapter as well as a Member of the Electromobility Board of the National Centre for Research and Development. His research focuses on issues linked with the assurance of power quality as well as the interoperability of power systems involving power electronic interfaces and control arrangements.

Piotr Lezynski (Senior Member, IEEE) received the M.Sc. degree in 2008 and the Ph.D. degree in 2014 in electrical engineering from the University of Zielona Gora, Zielona Gora, Poland.

During 2008–2010, he was a Designer of power electronics with the company Metrol in Zielona Gora. Since 2011, he has been with the Institute of Automatics, Electronics and Electrical Engineering, University of Zielona Gora. In addition to scientific and didactic work, he conducts commercial EMC measurements in the EMC Laboratory of the institute. His scientific interests include issues of EMC of power electronics devices.

Jacek Bojarski was born in 1968 in Kostrzyn, Poland. He received the M.Sc. and Ph.D. degrees in mathematical statistics from the Technical University of Zielona Gora, Zielona Gora, Poland, in 1996 and 2000, respectively.

He is a Teacher in the Division of Mathematical Statistics and Econometrics with the University of Zielona Gora. His major research interests include statistical, especially Bayesian, estimators, and uncertainty analysis. One of his research activities includes the utilization of advanced computer science technologies in mathematics.

David W. P. Thomas (Senior Member, IEEE) received the B.Sc. degree in physics from Imperial College, London, U.K., in 1981, the M.Phil. degree in space physics from Sheffield University, Sheffield, U.K., in 1984, and the Ph.D. degree in electrical engineering from Nottingham University, Nottingham, U.K., in 1990.

He is a Professor of electromagnetics applications with the George Green Institute for Electromagnetics Research, The University of Nottingham, Nottingham, UK.

He is a member of CIGRE and Convenor for Joint Working Group C4.31 EMC between communication circuits and power systems, Chair of COST Action IC 1407 "Advanced characterisation and classification of radiated emissions in densely integrated technologies," a member of several conference committees, and the EMC Europe International Steering Committee. His research interests include electromagnetic compatibility, electromagnetic simulation, power system transients, and power system protection.

Frede Blaabjerg (Fellow, IEEE) received the Ph.D. degree in electrical engineering from Aalborg University, Aalborg, Denmark, in 1995.

He was with ABB-Scandia, Randers, Denmark, from 1987 to 1988. He became an Assistant Professor in 1992, an Associate Professor in 1996, and a Full Professor of power electronics and drives in 1998. In 2017, he became a Villum Investigator. He is Honoris Causa at University Politehnica Timisoara, Romania, and Tallinn Technical University, Estonia. His current research interests include power electronics and its applications, such as in wind turbines, PV systems, reliability, harmonics, and adjustable speed drives.

He has published more than 600 journal papers in the fields of power electronics and its applications. He is the co-author of four monographs and editor of ten books in power electronics and its applications.

He has received 32 IEEE Prize Paper Awards, the IEEE PELS Distinguished Service Award in 2009, the EPE-PEMC Council Award in 2010, the IEEE William E. Newell Power Electronics Award 2014, the Villum Kann Rasmussen Research Award 2014, the Global Energy Prize in 2019, and the 2020 IEEE Edison Medal. He was the Editor-in-Chief of the IEEE Transactions on Power Electronics from 2006 to 2012. He has been Distinguished Lecturer for the IEEE Power Electronics Society from 2005 to 2007 and for the IEEE Industry Applications Society from 2010 to 2011 as well as 2017 to 2018. In 2019–2020, he serves a President of IEEE Power Electronics Society. He is Vice-President of the Danish Academy of Technical Sciences too. He is nominated in 2014-2019 by Thomson Reuters to be between the most 250 cited researchers in Engineering in the world.